DOI: 10.1002/chem.200700195

# A Sensitive Fluorescence Anisotropy Method for Point Mutation Detection by Using Core–Shell Fluorescent Nanoparticles and High-Fidelity DNA Ligase

**Ting Deng, Jishan Li, Jian-Hui Jiang,* Guo-Li Shen,* and Ru-Qin Yu[a]**

**Abstract:** The present study reports a proof-of-principle for a sensitive genotyping assay approach that can detect single nucleotide polymorphisms (SNPs) based on fluorescence anisotropy measurements through a core–shell fluorescent nanoparticles assembly and ligase reaction. By incorporating the core–shell fluorescent nanoparticles into fluorescence anisotropy measurements, this assay provided a convenient and sensitive detection assay that enabled straightforward single-base discrimination without the need of complicated operational steps. The assay was implemented via two steps: first, the hybridization reaction that allowed two nanoparticle-tagged probes to hybridize with the target DNA strand and the ligase reaction that generated the ligation between perfectly matched probes while no ligation occurred between mismatched ones were implemented synchronously in the same solution. Then, a thermal treatment at a relatively high temperature discriminated the ligation of probes. When the reaction mixture was heated to denature the duplex formed, the fluorescence anisotropy value of the perfect-match solution does not revert to the initial value, while that of the mismatch again comes back as the assembled fluorescent nanoparticles dispart. The present approach has been demonstrated with the discrimination of a single base mutation in codon 12 of a K-ras oncogene that is of significant value for colorectal cancers diagnosis, and the wild type and mutant type were successfully scored. Due to its ease of operation and high sensitivity, it was expected that the proposed detection approach might hold great promise in practical clinical diagnosis.

**Keywords:** DNA · fluorescence anisotropy · nanotechnology · single-nucleotide polymorphism

## Introduction

Single nucleotide polymorphisms (SNPs) are the most abundant form of genetic variation and occur once every 100–300 bases.[1] It is believed that many pathogenic and genetic diseases are associated with changes in the sequence of particular genes, and these genetic variations can serve as biomarkers for medical diagnosis at early stages of the diseases.[2] Thus it is required that diagnostic techniques being developed have the capability of identifying these mutations. Conventional procedures involved the employment of mass spectrometry or gel electrophoresis for the discrimination of fragments produced by endonuclease cleavage.[3,4] These methods are time-consuming and of relatively high cost. Current approaches used to detect SNP include primarily the allele-specific DNA microarray,[5,6] the allele-specific TagMan assay,[7] the template-directed dye terminator incorporation assay[8] and the ligase detection reaction.[9–11] Among these assays, the DNA enzyme-based approaches have attracted increasing interest due to its cost efficiency, ease of operation and rapidness of implementation. Moreover, the incorporation of DNA enzymes offers additional advantages of high fidelity and improved sensitivity.

Recently, based on the Mirkin's pioneering work,[12–14] we reported a convenient yet powerful colorimetric detection that enabled a straightforward single base discrimination without the need of precise temperature control through the gold nanoparticle assembly and the ligase reaction.[15] Because some reagents such as DTT would lead to the aggregation of Au nanoparticle probes, these reagents should be circumvented such that conditions for the ligase reaction in the reported study had to be made different from the ideal ones, which might induce a loss of the nick-closing activity of the enzyme. Moreover, due to strong electrostatic repul-

[a] Dr. T. Deng, Dr. J. Li, Prof. Dr. J.-H. Jiang, Prof. G.-L. Shen, Prof. R.-Q. Yu
State Key Laboratory of Chem/Biosensing and Chemometrics
Chemistry and Chemical Engineering College, Hunan University
Changsha 410082 (China)
Fax: (+86) 731-882-1355
E-mail: jianhuijiang@hnu.cn
glshen@hnu.c

   

sion between oligonucleotide-modified Au nanoparticles, the hybridization of template with Au–nanoparticle probe should be performed under high salt concentration, despite a lower salt concentration was required for the ligase reaction. This made the colorimetric detection protocol operationally complicated in that the hybridization was performed in high salt buffer and the ligase reaction was executed in diluted solution, possibly deteriorating the analytical accuracy of the point mutation detection.

In this paper, we focused on developing a novel detection system based on fluorescence anisotropy (FA) measurement that enabled a straightforward single base discrimination with a high fidelity Tth DNA ligase[16,17] through the assembly of novel core–shell near-infrared (NIR) fluorescent nanoparticles[18] and the ligase reaction. FA is a polarization-based technique that provides a quantitative measure for the rotational motion of a fluorescent molecule-linked object. In a particular surrounding, the rotational motion of the fluorescent molecule-linked object is closely related to the size of the object. For instance, when a fluorescence molecule is free in solution, it rotates at a rate commensurate with its size and the fluorescence anisotropy value is relatively small. If, however, the fluorescence molecule forms a complex with another substance, its rotational rate decreases and the fluorescence anisotropy value increases, the degree of variation depends on the strength of the binding interaction and the size of the complex.[19,20] The detection scheme is illustrated in Scheme 1. This assay uses an

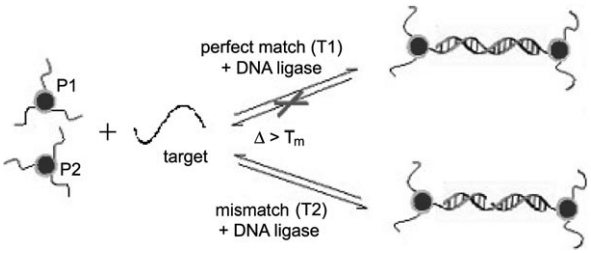


Scheme 1. Illustration of the fluorescent nanoparticle assembly and ligase reaction-based point mutation assay. The fluorescent nanoparticles were chemically modified with 3′- or 5′-(amino)oligonucleotides (probe). These probes flank a single-base mutation on the target template. High-fidelity DNA ligase covalently joins the two adjacent probes P1, P2 when both probes perfectly matched to the template, fluorescence anisotropy value of nanoparticles does not revert to the initial value after annealing. If there exist one mismatch with the template at the end of the allele-specific discriminating probe, the reversion of fluorescence anisotropy value would not occur.

allele-specific discriminating probe (P1) and a common probe (P2) that flank the mutation site and are both immobilized on the surface of core–shell near-infrared fluorescent nanoparticles. Hybridization of the target strand (T1 or T2) with the probes results in the formation of an extended polymeric fluorescent nanoparticle–polynucleotide aggregate, thus there is a measurable increase in the fluorescence anisotropy value of the oligonucleotide-labeled fluorescent nanoparticles. A perfect match between the base at the 3′-end of the discriminating probe and the target allows the ligase to covalently join the two adjacent probes flanking the mutation site, while a single-base mismatch does not. When the reaction mixture is heated to denature the formed duplex, fluorescence anisotropy value corresponding to the perfect-matched target does not revert to the initial value due to the covalent linkage between the discriminating and the common probes, while that associated with the mismatch turns back to the small initial value as the assembled fluorescent nanoparticles dispart. Therefore, point mutation in DNA target can be discriminated via such sensitive fluorescence anisotropy measurements. Compared with our previous work, the introduction of new fluorescence nanoparticle detection tag, the ligase reaction can be performed together with the hybridization in the ideal conditions thus this assay presented a more sensitive, specific, rapid and convenient detection method. In addition, the utilization of the novel core–shell near-infrared fluorescent nanoparticles offers the possibility of eliminating the endogenous fluorescence of biomolecules as well as the strong absorption of whole blood and tissue samples.

## Results and Discussion

**Characterization of core–shell NIR fluorescence nanoparticles**: The prepared core–shell NIR fluorescence nanoparticles were characterized by TEM and fluorescence spectroscopy. As shown in Figure 1a, one observes that the nanoparticles have a typical core–shell spherical structure. An average size of 65 nm with a standard deviation of 6 nm was estimated with 100 particles, indicating the reverse microemulsion system served as very uniform microreactors for the hydrolysis of silane reagents. The core–shell structure was derived naturally from the preparation procedure that involved two hydrolysis reactions, that is, a preliminary co-hydrolysis of a long-chain silicon alkoxide HDTMOS and TEOS to form a MB-doped hydrophobic core followed by the hydrolysis of TEOS to form a hydrophilic shell. Such a core–shell protocol was essential for the preparation of MB-based NIR fluorescence nanoparticles. The highly hydrophobic core was very efficient for entrapping the near-infrared dye and enhancing its fluorescence substantially. The hydrophilic shell enables the nanoparticles to be well dispersed in aqueous solution and improve its stability to quenching and leaching. Figure 1 depicts the fluorescence spectra of the nanoparticles. It is seen that the nanoparticle has a maximum excitation around 667 nm and an emission peak at 682 nm, both located in the NIR spectrum region. The indicated that our point mutation detection method based on assembly of NIR fluorescent nanoparticles offered the possibility of eliminating the endogenous fluorescence of biomolecules as well as the strong absorption of whole blood and tissue samples.

**Hybridization of wild-type or mutant template with fluorescent nanoparticle probes**: The salt concentration is one of

  

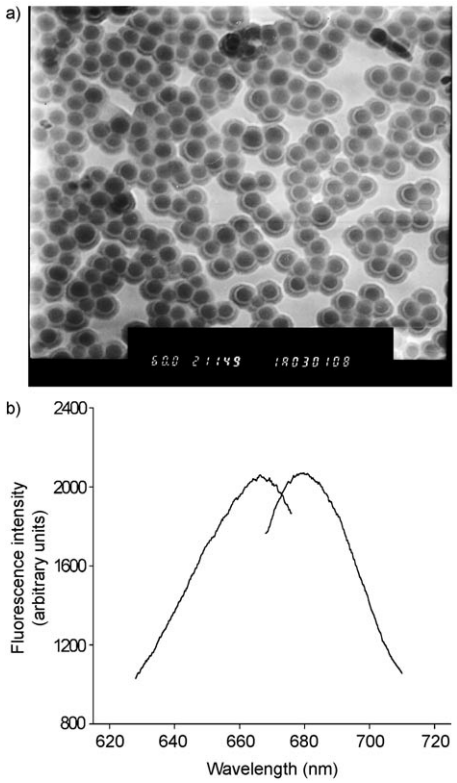


Figure 1. a) TEM image of the synthesized MB-doped core–shell fluorescent nanoparticles at 60000× magnification. b) Fluorescence spectra of MB-doped core–shell fluorescent nanoparticles.

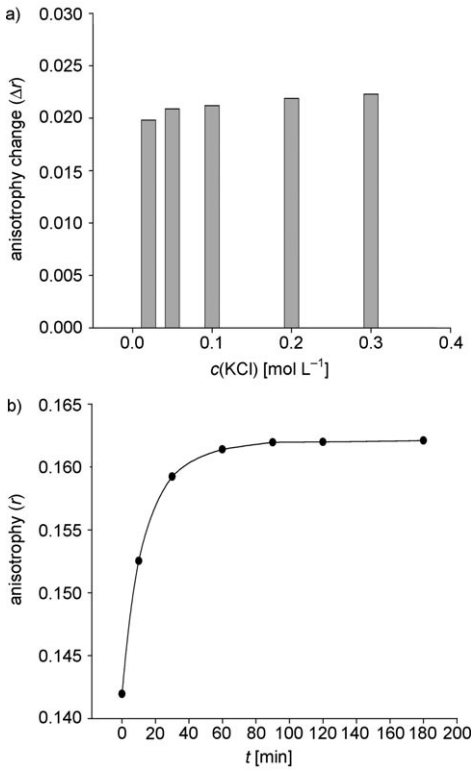


Figure 2. a) Effect of KCl concentration on hybridization of targets with nanoparticle probes. b) Effect of hybridization time between targets and fluorescent nanoparticle probes. The reaction mixture contains each fluorescent probe in 50 μL solution and 320 pM of oligonucleotide target. After mixing, the mixture was heated to 65 °C, followed by measuring the fluorescence anisotropy value of the resulting solution.

important factors affecting the hybridization of the template with probes. In our previous work,[15] we found, due to the strongly electrostatic effect between Au nanoparticles, the hybridization of template with Au nanoparticle probes could not be carried out even in 24 h when the hybridization was performed under a low concentration of KCl that is the optimal salt concentration for the ligase reaction. Thus, the effect of salt concentration on the hybridization of the template with fluorescent nanoparticle probes was investigated in this study first. The results are shown in Figure 2a. As can be seen, the hybridization of the template with fluorescent nanoparticle probes can be performed well under the KCl concentration range from 0.02 to 0.3 M. Thus, the hybridization of template with fluorescent nanoparticle probes and the ligase reaction can be carried out in the same buffer containing 0.05 M KCl, consequently the experimental operations are substantially simplified. In addition, as can be seen from Figure 2b, when the hybridization of template with fluorescent nanoparticle probes was performed in 0.05 M KCl Tris-HCl buffer, the DNA sequence recognition can be completed within about 60 min. Thus 60 min was selected as the hybridization time in the following experiments.

**Melting analysis**: The thermal ligase was shown to have the optimal nick-closing activity at a temperature about 65 °C.[11] Therefore, it is essential to ensure the duplex formed between the nanoparticle-tagged probes and the template does not dissociate at such a temperature. Otherwise, the ligation reaction would not be taking place. Thus, the melting analysis of the duplex was investigated. The results are shown in Figure 3. The melting curve clearly reveals that the anisotropy value of fluorescent nanoparticle aggregates show a substantial alteration at about 70 °C. Thus, the melting temperatures ($T_m$) of the duplex is about 70 °C indicating that the duplex formed between the nanoparticle-tagged probes and the template (T1) does not dissociate at 65 °C. Therefore, for the appropriately designed probes, the hybridization and ligation reactions were performed consistently at 65 °C in the present detection procedure.

**Ligation detection of wild-type or mutant target using fluorescent nanoparticle probes**: When the template does not perfectly match with fluorescent nanoparticle probes, the nick between the two adjacent probes would not be closed by ligase. Hence, the fluorescence anisotropy value of detection tags would revert to the initial one after denaturing at a temperature, say 80 °C, higher than the melting point. On the contrary, a perfect match between the base at the 3′-end of the discriminating probe and the target allows the ligase to covalently join the two adjacent probes that flanked the mutation site. Therefore, when the reaction mixture is heated to denature the duplex formed, fluorescence aniso-

  

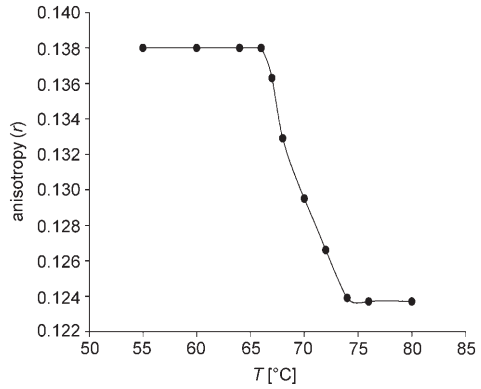


Figure 3. Melting analysis of the duplex formed between the nanoparticle-tagged probes and the template. The reaction mixture contains each fluorescent probe in 50 μL solution and 150 pM of oligonucleotide target. After mixing, the reaction mixture was heated to 65 °C for 60 min. Then, the melting analysis was performed via monitoring the fluorescence anisotropy value at increasing temperature.

tropy value of the perfect match sample does not revert to the initial value. The fluorescent anisotropy changes of the perfect match and single-base mismatch samples in different conditions are shown in Figure 4. For the perfect match, the anisotropy value has not obvious decrease after denaturing the duplex formed, while the anisotropy value for the single-base mismatch reverts to the initial value after denaturing the duplex formed. Thus, the single-point mutation can be discriminated via the sensitive fluorescence anisotropy detection system based on the fluorescent nanoparticles assembly and the ligase reaction. Moreover, for the single-base mismatch target, we repeated the hybridization and denaturation steps for five times, reproducible fluorescence anisotropy changes were obtained, indicators that the nanoparticle probes were sufficiently stable to thermal treatment involved in the experiments.

**Quantitative analysis of the target gene concentration using fluorescence anisotropy assay**: Due to that hybridization of the target strand with the probes results in a measurable increase in the fluorescence anisotropy value of the oligonucleotide-labeled fluorescent probes, the target gene containing a single-base mutation, that is, the perfect matched target, can be quantified. As observed in Figure 5 the fluorescence anisotropy is dynamically correlated to the target concentration in the range from 320 fM to 3.2 nM. Compared with our previous work, the detection limit is distinctly improved, which might be attributed to the application of sensitive fluorescence anisotropy assay and the optimal reactive conditions of the ligation.

**Analysis of genomic DNA**: In order to show that the developed method was applicable to real samples, the PCR products of HT29 and SW480 genomic DNA were detected using the developed fluorescence anisotropy assay method. The gel electrophoresis image of the two PCR products confirmed the length of these two sequences is 254 bp. Analytical results of the two samples using the fluorescence anisotropy assay method are shown in Figure 6. One observes that, after denaturing at a melting temperature, the fluores-

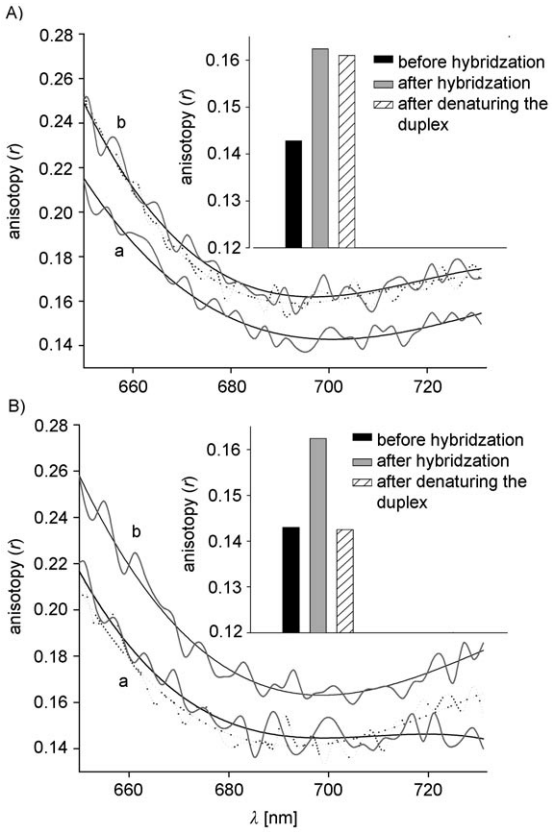


Figure 4. Discrimination of mutant target (A, T1) and wild-type target (B, T2) by fluorescence anisotropy assay. Solid line a, before hybridization; Solid line b, after hybridization; dashed line, denaturing after ligation. The inset is obtained from its relative fluorescence anisotropy spectrum. The reaction mixture contains 50 μL of each fluorescent probe solution, 320 pM of oligonucleotide target and 0.05 U μL of Tth DNA ligase. The experiments were carried out as described in experimental section.

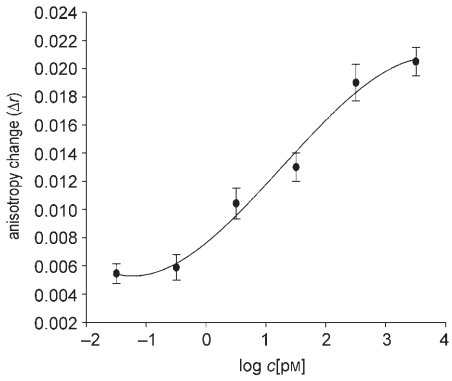


Figure 5. Quantitative analysis of the target gene concentration using fluorescence anisotropy assay based on the self-synthesized fluorescent nanoparticle probes. The experiments were carried out as described in Experimental Section. The standard deviations obtained by five repeated measurements are shown as the error bars.

  

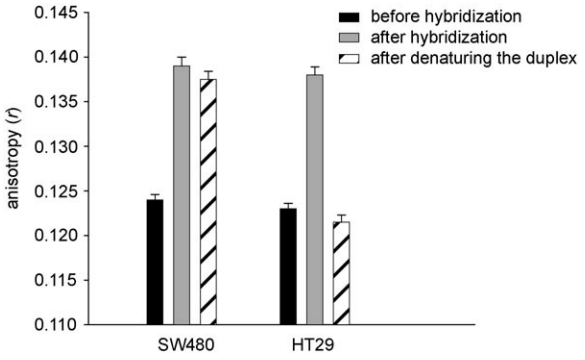


Figure 6. Assay of two real gene samples (SW480 and HT29) by using the fluorescence anisotropy method.

cence anisotropy value for HT29 sample recovers to the initial value, indicating there is no point mutation in codon 12 in HT29 genomic DNA. On the contrary, the fluorescence anisotropy value for SW480 sample exhibits insignificant variations after denaturing at a melting temperature and almost reverts to the initial value. This implies that the nick between the two adjacent probes was not sealed at the joining site for SW480. That is to say, the codon 12 of K-ras gene has a point mutation. These results were further verified by the sequencing data (data not shown). The results that the codon 12 for HT29 and SW480 genomic DNA are GGT (the 84th base in the PCR product) and GTT (the 92nd base in the PCR product), respectively, implying that there is no mutation at codon 12 for HT29, and codon 12 for SW480 is mutant from GGT to GTT. These results demonstrate that the developed method holds great promise in rapid point mutation detection of real genomic DNA samples.

## Conclusion

The present study reported a novel detection system based on fluorescence anisotropy measurement that enabled a straightforward detection and quantification of target gene containing SNP through the high fidelity perfect-match ligation of DNA ligase and the core–shell fluorescent nanoparticles assembly. And the fluorescent nanoparticles as detection tags are immune from the reagents that lead to the aggregation of Au–nanoparticle probes in our previous work but offer the help to the nick-closing activity of the enzyme. Thus, the ligase reaction can be performed in the optimal conditions and the sensitivity of the present assay approach is significantly improved. This new, fluorescent nanoparticle assembly and ligase reaction based detection procedure may prove useful in clinical diagnosis of genetic diseases that contain single nucleotide mutations.

## Experimental Section

**Materials**: All oligonucleotides (see Table 1) and the DNA ligase buffer containing 0.05 M KCl, 20 mM Tris-HCl (pH 8.3), 10 mM $MgCl_2$, 1 mM EDTA, 1 mM $NAD^+$, 10 mM DTT and 0.1 % v/v Triton X-100 were obtained from Takara Biotechnology Co., Ltd (Dalian, China), and were used as received. Thermal ligase (Tth DNA ligase) was obtained from ABgene (UK). Tris was obtained from Roche. NaCl, KCl and $MgCl_2$ were purchased from Amresco (Solon, America). Cyclohexane, *n*-hexanol, and ammonium hydroxide (25–28 wt %) were obtained from National Reagent Corporation (Shanghai, China). Tetraethyl orthosilicate (TEOS) was purchased from Wulian Chemical Factory (Shanghai, China). Methylene blue (MB) was obtained from Sigma. Hexadecyltrimethoxysilane (HDTMOS) was purchased from Fluka. 3-[2-(2-Aminoethylamino)ethylamino]propyltrimethoxysilane (AEAPTMS) was obtained from Acros. Deionized water was obtained through a Nanopure Infinity ultrapure water system (Barnstead/thermolyne Corp, Dubuque, America) and had an electric resistance $>18.3\,M\Omega$.

Table 1. Synthesized oligonucleotides used in this experiment.[a]

| |
|---|
| probe 1 (P1) 5′-$NH_2$-$(CH_2)_6$- TAAAA CTT GTG GTA GTT GGA GCT G**T**-3′ |
| probe 2 (P2) 5′-pT GGC GTA GGC AAG AGT GCC CT-$(CH_2)_6$-$NH_2$ −3′ |
| target 1 (T1) 3′-TTTT GAA CAC CAT CAA CCT CGA C**A**A CCG CAT CCG TTC TCA CGG G-5′ |
| target 2 (T2) 3′-TTTT GAA CAC CAT CAA CCT CGA CCA CCG CAT CCG TTC TCA CGG G-5′ |

[a] Targets and probes were designed according to ref. [2] with some modifications for detecting point mutation in codon 12 of K-ras gene associated with colorectal cancer. In this mutation, the second site in codon 12, GGT, coding for glycine, mutates to GTT coding for valine. The framed bases in P1 and T1 indicate the point mutation. p in P2 represents phosphate moiety at 5′ end.

**Preparation and surface modification of core–shell fluorescent nanoparticles**: The nanoparticles were prepared using the microemulsion method as reported in our previous study[18] and briefly described as follows: Triton X-100 (21.30 g) and *n*-hexanol (20 mL) were added to cyclohexane (80 mL), followed by stirring of the mixture for 15 min. The MB solution (6.5 mL, 0.0025 mol $L^{-1}$) was added into the mixture, and a transparent and stable reverse microemulsion was obtained after several-minute stirring. After continuous stirring for 15 min, a freshly prepared mixture of TEOS/HDTMOS 1:3 and $NH_4OH$ solution (2 mL) were successively added to the reverse microemulsion system under vigorous stirring. The reaction mixture was stirred continuously for 24 h at room temperature, which resulted in the formation of the MB-doped core particles after the hydrolysis of the silane mixture. Then, TEOS (2 mL) and $NH_4OH$ (1 mL) were added to the microemulsion solution and the hydrolysis reaction was allowed to proceed again under constant stirring for another 24 h. After completion of the reaction, the MB-based core–shell fluorescent nanoparticles were obtained. With reverse microemulsion system collapsed by addition of acetone (10 mL), the nanoparticles were isolated by centrifugation and washed with ethanol (3×) and then water (3×) to remove any surfactant. During each washing, the solution was sonicated sufficiently to disperse the nanoparticles. The resulting fluorescent nanoparticles were characterized using transmission electron microscope (TEM, Hitachi 800, Japan) and spectrofluorometer (Jobin Yvon Fluorolog-3, France).

The surface modification of nanoparticles with AEAPTMS was performed as follows: Appropriate amount of nanoparticles (8 mg, about $2.1\times10^{13}$ nanoparticles) was dispersed in anhydrous ethanol (20 mL), then AEAPTMS (0.4 mL) was added. The reaction was allowed to proceed for 1 h under stirring. After centrifugation, the nanoparticles were washed with ethanol and water (3×). The amino-modified fluorescent nanoparticles were thus obtained for subsequent modification of oligonucleotide probe.

  

**Preparation of oligonucleotide-modified fluorescent nanoparticles**: The amino-modified nanoparticles were suspended in 5% glutaraldehyde solution (5 mL) for 2 h under stirring. After centrifugation, the surface-modified nanoparticles were washed with water (3×) and then suspended in 0.06 mol $L^{-1}$ phosphate buffer (1 mL; pH 7.4). To modify the nanoparticles with oligonucleotide probe P1 with amino moiety at the 5′ end, an aqueous solution of P1 (50 μL, 12 nmol) was added into the solution under stirring. After stirring for 4 h, a glycine solution (50 μL, 0.1 M) was added into the mixture and stirred for 1 h to block free -CHO groups. After centrifugation and washing with 20 mM Tris-HCl (pH 8.3) solution containing 0.05 M KCl, the P1-modified fluorescent nanoparticles were dispersed in the DNA ligase buffer solution and stored at 4°C before use. The modification of nanoparticles using oligonucleotide probe P2 with amino moiety at 3′ end was performed in a manner described above via replacing P1 by P2, and the P2-modified fluorescent nanoparticles were also dispersed in the DNA ligase buffer solution and stored at 4°C before use.

**Point mutation detection**: In a typical experiment, the appropriate oligonucleotide target was added to 100 μL of fluorescent nanoparticle probes solution containing 50 μL of each fluorescent probe. After mixing, 5.12 U of the Tth DNA ligase was added and the reaction mixture was heated to 65°C for 60 min, followed by the fluorescence anisotropy measurement of the resulting solution using a spectrofluorometer (Jobin Yvon Fluorolog-3, France) at a constant temperature (25°C). Finally, after 5 min of denaturing at 80°C, the solution was rapidly immersed in ice water and then the fluorescence anisotropy measurement of the resulting solutions was again performed at the constant temperature.

**Genomic DNA extraction and PCR amplification**: Genomic DNA was extracted from cell lines HT29 (wildtype) and SW480 (mutant, CD 12 GGT→GTT). The cell lines were cultured at 37°C in RPMI 1640 (GIBCO BRL) with 10% fetal calf serum (FCS) and 100 U $mL^{-1}$ penicillin/streptomycin. Harvested cells (ca. $10^7$) were suspended in a DNA extraction buffer containing 10 mM Tris-HCl (pH 7.5), 150 mM NaCl, 2 mM EDTA (pH 8.0), 0.5% SDS and 200 μ per mL proteinase K followed by the incubation at 37°C for 24 h. The samples were centrifuged, and EtOH in three-fold volume was added to precipitate the DNA extract from the supernatant. The precipitated DNA was washed with 70% EtOH and resuspended in TE buffer (10 mM Tris-HCl, pH 7.5 and 2 mM EDTA, pH 8.0).

The PCR amplification was performed with genomic DNA (about 40 ng) extracted from the cell lines in Tris-HCl buffer (50 μL, 10 mM, pH 8.3) containing 10 mM KCl, 4.0 mM $MgCl_2$, 250 μM dNTPs, as well as 1 μM forward and reverse primers. The forward primer was 5′-AACCTTATGTGTGACATGTTCTAATATAGTCAC-3′, the reverse 5′-AAAATGGTCAGAGAAACCTTTATCTGTATC-3′. Amplification was achieved by thermal cycling for 40 times with denaturing at 95°C for 30 s, annealing at 60°C for 30 s and extension at 72°C for 1 min, with a final extension at 72°C for 10 min followed after the thermal cycling. PCR products were purified by Agar Gel DNA Purification Kit (GIBCO BRL). The purified PCR products were denatured at 90°C for 10 min and rapidly immersed in ice water to allow for hybridization with nanoparticle probes.

## Acknowledgements

This work was financially supported by the National Natural Science Foundation of China (Grant No. 20435010, 20575020, U0632005) and Ministry of Education (NCET-04-0768).

[1] R. Sachidanandam, D. Weissman, S. C. Schmidt, J. M. Kakol, L. D. Stein, G. Marth, S. Sherry, J. C. Mullikin, B. J. Mortimore, D. L. Willey, *Nature* **2001**, *409*, 928–933.
[2] M. B. Wabuyele, H. Farquar, W. Stryjewski, R. P. Hammer, S. A. Soper, Y. W. Cheng, F. Barany, *J. Am. Chem. Soc.* **2003**, *125*, 6937–6945.
[3] P. Ross, L. Hall, I. Smirnov, L. Haff, *Nat. Biotechnol.* **1998**, *16*, 1347–1351.
[4] D. Schmalzing, A. Belenky, M. A. Novotny, L. Koutny, O. Salas-Solano, S. El-Difrawy, A. Aram, P. Matsudaira, D. Ehrlich, *Nucleic Acids Res.* **2000**, *28*, e43.
[5] D. G. Wang, J. B. Fan, C. J. Siao, A. Berno, P. Young, R. Sapolsky, *Science* **1998**, *280*, 1077–1082.
[6] J. G. Hacia, *Genome Res.* **1998**, *8*, 1245–1258.
[7] K. J. Livak, J. Marmaro, A. J. Todd, *Nat. Genet.* **1995**, *9*, 341–342.
[8] X. Chen, Y. P. Kwok, *Nucleic Acids Res.* **1997**, *25*, 347–353.
[9] V. O. Tobe, S. L. Taylor, D. A. Nickerson, *Nucleic Acids Res.* **1996**, *24*, 3728–3732.
[10] U. Landegren, R. Kaiser, J. Sanders, L. Hood, *Science* **1988**, *241*, 1077–1080.
[11] F. Barany, *Proc. Natl. Acad. Sci. USA* **1991**, *88*, 189–193.
[12] C. A. Mirkin, R. L. Letsinger, R. C. Mucic, J. J. Storhoff, *Nature* **1996**, *382*, 607–609.
[13] R. Elghanian, J. J. Storhoff, R. C. Mucic, R. L. Letsinger, C. A. Mirkin, *Science* **1997**, *277*, 1078–1081.
[14] J. J. Storhoff, R. Elghanian, R. C. Mucic, C. A. Mirkin, R. L. Letsinger, *J. Am. Chem. Soc.* **1998**, *120*, 1959–1964.
[15] J. S. Li, X. Chu, Y. L. Liu, J. H. Jiang, Z. M. He, Z. W. Zhang, G. L. Shen, R. Q. Ru, *Nucleic Acids Res.* **2005**, *33*, e168.
[16] J. Y. Luo, D. E. Bergstrom, F. Barany, *Nucleic Acids Res.* **1996**, *24*, 3071–3078.
[17] J. Tong, W. G. Cao, F. Barany, *Nucleic Acids Res.* **1999**, *27*, 788–794.
[18] T. Deng, J. S. Li, J. H. Jiang, G. L. Shen, R. Q. Yu, *Adv. Funct. Mater.* **2006**, *16*, 2147–2155.
[19] M. E. McCarroll, F. Haddadian Billiot, I. M. Warner, *J. Am. Chem. Soc.* **2001**, *123*, 3173–3174.
[20] N. J. Gibson, H. L. Gillard, D. Whitcombe, R. M. Ferrie, C. R. Newton, S. Little, *Clin. Chem.* **1997**, *43*, 1336–1341.

Received: February 4, 2007
Published online: July 2, 2007

  